

Atmospheric electricity coupling between earthquake regions and the ionosphere

R.G. Harrison ⁽¹⁾, K.L. Aplin ⁽²⁾ and M.J. Rycroft ⁽³⁾

(1) Department of Meteorology, University of Reading, Earley Gate, Reading RG6 6BB, UK

(2) Space Science and Technology Department, Rutherford Appleton Laboratory, Chilton, Didcot, Oxon OX11 0QX, UK

Now at Physics Department, University of Oxford, Denys Wilkinson Building, Keble Road, Oxford OX1 3RH, UK

(3) CAESAR Consultancy, 35 Millington Road, Cambridge, CB3 9HW, UK,

and Centre for Space, Atmospheric and Oceanic Sciences, University of Bath, Bath BA2 7AY, UK

accepted for publication in Journal of Atmospheric and Solar-Terrestrial Physics

J. Atmos Solar Terr Physics 72, 376-381 (2010) <http://dx.doi.org/10.1016/j.jastp.2009.12.004>

Abstract

We propose a mechanism to explain suggested links between seismic activity and ionospheric changes detected overhead. Specifically, we explain changes in the natural extremely low frequency (ELF) radio noise recently observed aboard the DEMETER satellite at night, before major earthquakes. Our mechanism utilises increased electrical conductivity of surface layer air before a major earthquake, which reduces the surface-ionosphere electrical resistance. This increases the vertical fair weather current, and (to maintain continuity of electron flow) lowers the ionosphere. Magnitudes of crucial parameters are estimated and found to be consistent with observations. Natural variability in ionospheric and atmospheric electrical properties is evaluated, and may be overcome using a hybrid detection approach. Suggested experiments to investigate the mechanism involve measuring the cut-off frequency of ELF “tweaks”, the amplitude and phase of VLF radio waves in the Earth-ionosphere waveguide, or medium frequency radar, incoherent scatter or rocket studies of the lower ionospheric electron density.

Keywords

Seismic precursors, troposphere-ionosphere coupling, conduction current density, radon, global circuit

1. Introduction

Earthquakes fall within the class of high impact natural events which can have substantial and tragic consequences for human populations. Reliable methods for earthquake prediction are therefore of massive potential benefits to society, but the suggested techniques remain in their infancy and may lack a rigorous theoretical basis. Some observations have suggested that changes in the ionosphere occur before earthquakes, but these effects are not yet well enough understood to be used for predictive purposes (e.g., Kim et al, 1994; Pulinets, 1998). However, recent results from the DEMETER satellite indicate a change of the radio noise spectrum¹, with a ~ 3 dB decrease of ELF wave intensity at 1.6-1.8 kHz, which can be explained by an increase of the cut-off frequency for propagation in the Earth-ionosphere waveguide at night, and which has been associated with earthquakes with magnitudes greater than 5.0 at depths less than 40 km (Nemec et al., 2009).

¹ The usually accepted definition of extremely low frequency, ELF, is 3Hz – 3 kHz, and very low frequency, VLF, 3 – 30 kHz.

Pre-seismic atmospheric electricity changes are one of the many possible predictive effects that have been noted. For example, a decrease in the atmospheric Potential Gradient (PG) near the Earth's surface, typically 100Vm^{-1} in undisturbed weather conditions, has been observed before some earthquakes (Kondo, 1968), and uncalibrated fluctuations in a corona current probe have also been attributed to pre-seismic PG changes (Kamogawa et al., 2004). Radon emissions from the ground, which cause air ionisation, increased before the 1995 Kobe earthquake, by up to an order of magnitude (Yasuoka and Shinogi, 1997; Yasuoka et al., 2006). An increase of the electrical conductivity of surface air due to radon emissions, or ions emitted from rock stresses (Freund et al, 2009) is consistent with a reduction of the PG, as explained by Pierce (1976).

Coupling between surface changes and upper atmosphere effects, suggested again by the DEMETER results, has remained troublesome to explain. Ionospheric changes have been associated with events originating in the lower troposphere, such as thunderstorms (Davis and Johnson, 2005), so earthquakes have been suggested to cause a similar coupling between the lower and upper atmosphere (reviewed by Rycroft, 2006). Kamogawa (2006) and Hayakawa (2006) summarised three possible candidate coupling mechanisms as follows:

1. Gases released from the ground during motions before the major earthquake shock modulate the properties of the entire atmosphere.
2. Ground motions excite atmospheric gravity waves that propagate upwards.
3. Electromagnetic radiation produced by processes acting in the ground before earthquakes initiate ionospheric effects.

The majority of the more persuasive existing observations fit within one of these frameworks, which are summarised in Table 1. However, there has been hitherto no theory which convincingly explains the linkage of pre-seismic surface changes to the ionosphere.

Table 1 Summary of proposed surface-ionosphere coupling mechanisms

Mechanism	Supporting observation	Example references
<i>Pre-seismic emissions:</i> Rock motions stimulate emissions that ultimately affect the total electron density in the ionosphere	Atmospheric electric field variations	Kondo (1968), Kamogawa et al. (2004)
	Changing infra-red emissions from surface, suggesting release of gas	Surkov et al. (2006)
	Over-the-horizon VHF emissions, suggesting changed properties of air	Hayakawa et al. (2007), Yonaiguchi et al. (2007)
	Total ionospheric content variations	Naman et al. (2002)
	Emission of ions from rock stresses	Freund et al (2009)
<i>Acoustic:</i> Excitation of atmospheric oscillations propagating upwards to the ionosphere	F-region ionospheric effects attributed to gravity waves	Hegai et al. (2006)
<i>Electromagnetic:</i> Direct emission of radio waves before the earthquake	VLF radio anomalies	Fujiwara et al. (2004), Ohta et al. (2002), Schekotov et al. (2007)
	UHF/VHF telemetry disturbances	Nagamoto et al. (2008)

We suggest here a simple mechanism coupling pre-seismic radon emanations to the electron density in the lower ionosphere. The coupling occurs through changes of the downward-directed conduction current density flowing in the global atmospheric electrical circuit in fair weather regions (Rycroft et al. 2000; Rycroft et al., 2007). Local modulation of the conduction current density can arise through changes in the surface layer air conductivity, associated here with seismic variations in the emission of radioactive gases from the Earth's crust. The continuous nature of the conduction current allows coupling to the ionosphere of surface radioactivity changes, from which changes in the local rate of charge transfer to the ionosphere will result. Figure 1 depicts the proposed coupling concept.

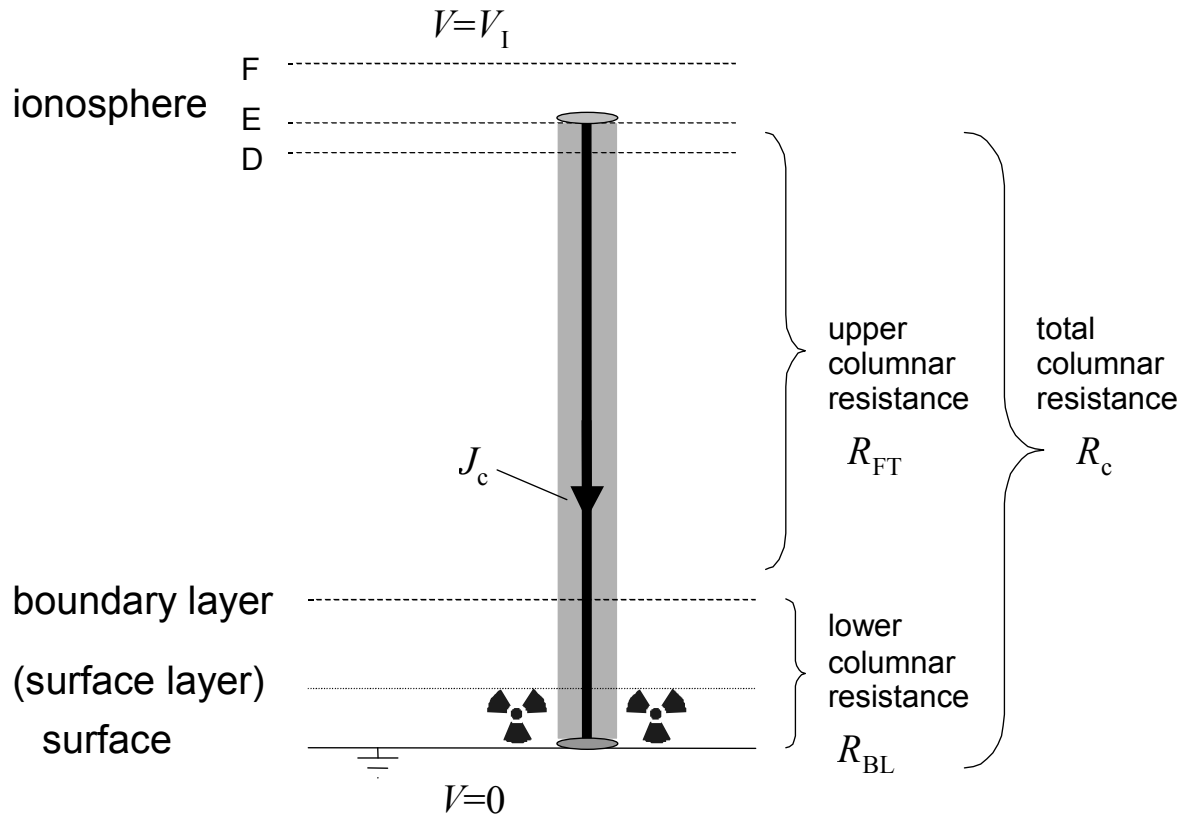


Figure 1. Conceptual model of the effect of surface layer air conductivity changes on the current flowing between the ionosphere and the Earth's surface. A local current density J_c flows between the ionosphere and the surface in fair weather regions, as a result of the potential difference V_I between the ionosphere and the surface, maintained by generators in the global atmospheric electrical circuit. The local current flowing depends on the local columnar resistance R_c , which has significant contributions from the lowest atmosphere and the free troposphere (FT), and a small ($\sim 7\%$) contribution from the stratosphere. Changes in the resistance of the atmospheric boundary layer (BL), through the release of radioactive gases into the surface layer, modify the total columnar resistance, and hence modify the conduction current flowing. This modifies the charge transferred to and from the ionosphere.

2. Surface layer conductivity effects on atmospheric electricity

The global atmospheric electrical circuit links charge separation in disturbed weather regions with current flow in fair weather regions (Rycroft et al., 2000, 2007). This occurs as a result of current flow through the ionosphere and the Earth's surface, which, in relation to the atmosphere in between, present upper and lower boundaries of relatively high electrical conductivity (Rycroft et al., 2008). The ionosphere at $\sim 80\text{km}$ altitude is typically maintained at a positive potential of $\sim 250\text{kV}$ with respect to the surface by the integrated effect of disturbed weather activity globally, such as thunderstorms and shower clouds. Finite conductivity of atmospheric air leads to a small "conduction" current density (J_c) flowing

between the surface and the ionosphere in fair weather conditions, which is typically $\sim 2 \text{ pA m}^{-2}$. The current density flowing locally is determined by the ionospheric potential V_I and the electrical resistance of the vertical column of atmosphere between the surface and the ionosphere. The resistance of a unit area atmospheric column is known as the columnar resistance, R_c , which is $\sim 100 - 170 \text{ P}\Omega \text{ m}^2$ (Rycroft et al., 2008).

(a) *Surface contributions to the columnar resistance*

Of the total atmospheric columnar resistance R_c , most of the resistance is contributed by the boundary layer (generally that region of atmosphere up to about $\sim 2 \text{ km}$ above the surface), R_{BL} . A further one-third is contributed above the boundary layer, from the free troposphere (FT), as R_{FT} ; this is regarded here to include the small ($\sim 7 \%$) stratospheric contribution. Changes in R_{BL} will arise from near-surface aerosol and radioactivity fluctuations; because of the dominance of R_{BL} in R_c , the surface effects have an appreciable effect on R_c . For low turbulence conditions, Harrison and Bennett (2007) proposed a linearised representation of the surface effects on R_c as

$$R_c = \frac{k}{\sigma_s} + R_{FT} \quad (1),$$

where σ_s is the conductivity of air in the surface layer having a height scale k . k is expected to be somewhat dependent on the climatology of the site concerned, as shallow surface layers have the least effect on R_c and well-mixed deep layers appreciably affect R_c (Anderson, 1977). At the relatively polluted Met Office site at Kew Observatory, near London, where long-term measurements of atmospheric electrical parameters were made, $k \sim 268 \text{ m}$, $R_{FT} = 93 \text{ P}\Omega \text{ m}^2$ and $R_c = 137 \text{ P}\Omega \text{ m}^2$ (Harrison and Bennett, 2007). The k value for Kew is probably appropriate to a densely populated urban site for which earthquake prediction would be required. For an ionospheric potential V_I , the conduction current density J_c is given by equation (1) using Ohm's Law as

$$J_c = \frac{V_I}{R_c} = V_I / \left[\frac{k}{\sigma_s} + R_{FT} \right] \quad (2),$$

which relates J_c and σ_s . From equation (2) it is clear that changes in the surface layer conductivity σ_s will also affect J_c , for constant V_I .

Such an effect of σ_s on J_c is evident in fair weather daily measurements from the Met Office site at Kew made over a long period using apparatus originally invented by C.T.R. Wilson (Harrison and Ingram, 2005). Data from the Wilson apparatus from 1966 to 1979, when the Kew Observatory closed, are shown in Figure 2. The Wilson σ_s and J_c values measured at the same site are correlated, which is evident from the locally-weighted statistical fit line (Cleveland, 1981). A further fitted line corresponding to equation (2) has been added, as equation (2) is used for subsequent estimations. This shows that, in the relatively clean air conditions leading to larger air conductivities, the simple theory underpinning equation (2) is probably conservative in the J_c response to σ_s which it estimates. The actual variations of σ_s are likely to have been caused by urban air pollution changes at Kew on the annual cycle of summer/winter air pollution. Surface air conductivity changes in other circumstances could also result from changes in ionisation rates, such as from fluctuations in radioactive gas concentrations.

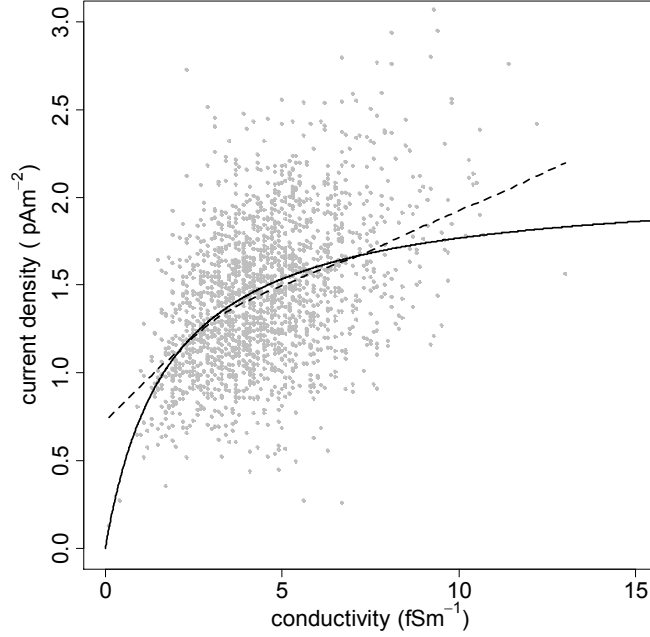


Figure 2. Daily fair weather measurements made at Kew over 14 years, of the conduction current density J_c and air conductivity σ_s . These were derived from independent Wilson apparatus measurements of J_c and the Potential Gradient, using Ohm's Law. A locally-weighted (LOWESS) fit line has been added (dashed line), and the expression of Harrison and Bennett (2007) fitted (solid line).

(b) Surface layer air conductivity

The lower part of the atmospheric boundary layer, the surface layer, contains particles and radioactive gases, which remove and produce ions, respectively. The electrical conductivity of surface layer air depends on the ion number concentration, for which the steady-state value is established by a balance between ion production and loss to aerosols (e.g., Harrison and Carslaw, 2003). The total air conductivity is the sum of the conductivity from both positive and negative ions. Using the ion balance equation, the total surface air conductivity σ_s is given by

$$\sigma_s = 2n\mu e = \mu e \frac{\left[\sqrt{(\beta^2 Z^2 + 4\alpha q)} - \beta Z \right]}{\alpha} \quad (3),$$

where n is the mean small ion number concentration, μ is the mean ion mobility ($1.2 \times 10^{-4} \text{ m}^2 \text{ V}^{-1} \text{ s}^{-1}$), α the ion-ion recombination coefficient ($1.6 \times 10^{-12} \text{ m}^3 \text{ s}^{-1}$), e is the magnitude of the charge on the electron, Z is the monodisperse aerosol number concentration and β is the ion-aerosol attachment coefficient, which is $\sim 4 \times 10^{-11} \text{ m}^3 \text{ s}^{-1}$ for $0.2 \text{ }\mu\text{m}$ radius aerosol (Harrison and Carslaw, 2003). (Ion mobility variation is small in comparison with ion concentration changes (Harrison and Tammet, 2008).) The ion production rate q at continental surfaces is usually assumed to be $10^7 \text{ m}^{-3} \text{ s}^{-1}$; about 40% of this is due to radon (Chalmers, 1967).

The response of σ_s to q from equation (3) is shown in figure 3a, in clean and polluted air, as considered previously by Pierce (1976). The sensitivity is approximately linear in polluted air, as the non-linear ion-ion recombination loss term is swamped by the linear ion-aerosol attachment loss term.

(c) Surface layer conductivity effects on conduction current density

Equations (1) and (3) can be combined to find the sensitivity of the conduction current to surface changes in radon concentration. Figure 3b shows the results of a related calculation, but using the parameters previously found for Kew, and assuming that $V_1 = 250$ kV. The radon ion production has been scaled to show a range of values, assuming that the typical ion production from radon is $4 \times 10^6 \text{ m}^{-3} \text{ s}^{-1}$.

Radon-induced surface layer air conductivity changes can therefore modify the columnar resistance sufficiently to have an appreciable effect on the conduction current. This effect is greatest in polluted surface air, which has the greatest proportional sensitivity of air conductivity to ion production rate changes. In polluted air, J_c increases approximately linearly with increasing radon ion production; doubling the radon ion production increases J_c by about 10%.

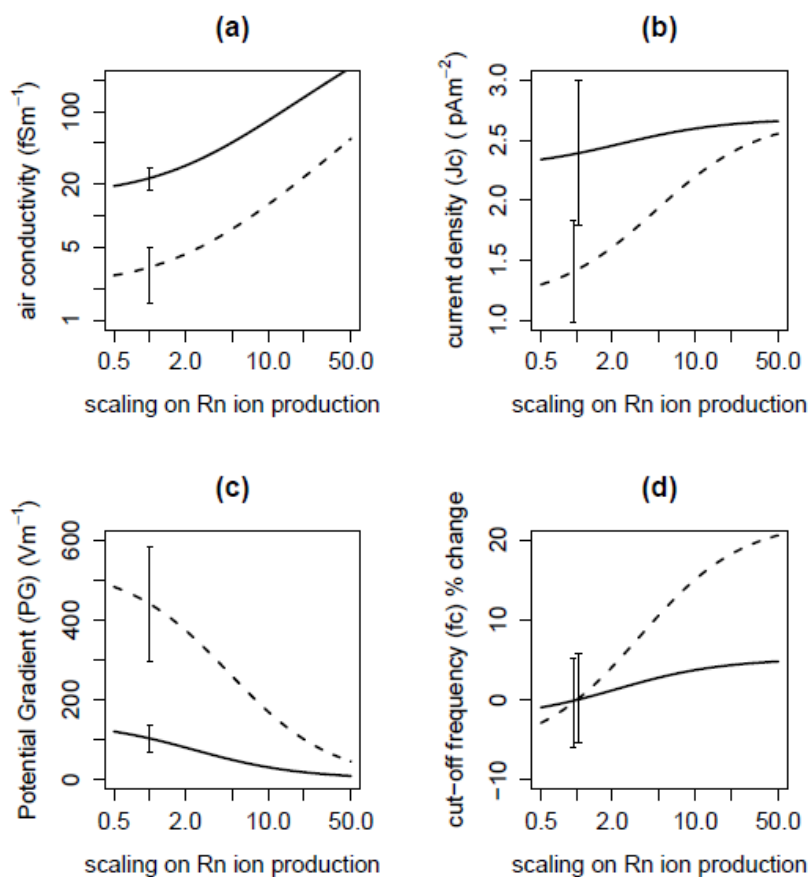


Figure 3. Responses of atmospheric electrical parameters to changes in the production of surface layer radon ionisation. (A value of 1.0 corresponds to 4×10^6 ions m^{-3} .) (a) Total air conductivity at the Earth's surface. (b) Conduction current density J_c . (c) Potential Gradient. (d) Percentage change in the ionospheric cut-off frequency (f_c) twelve hours after the surface radon change, through thickening of the lower ionosphere by upwards negative electron migration. Solid lines represent clean air (200 particles cm^{-3} of $0.25 \mu\text{m}$ radius), and dashed lines polluted air (1500 particles cm^{-3} of $0.25 \mu\text{m}$ radius). (Surface isoconductive layer thickness assumed as 268m.) Error bars for (a) to (c) are one standard deviation in long-term daily measurements from the UK geophysical observatories at Lerwick ("clean") and Kew ("polluted"); for (d) the peak to peak variability assumed is 10%.

3. Ionospheric response to conduction current density changes

The conduction current density J_c is constant with height between the surface and the ionosphere (Chalmers, 1967); therefore, changes in J_c due to surface layer air conductivity effects are directly communicated to the ionosphere. In the ionosphere, the conduction current density is primarily due to the motion of electrons, which are highly mobile in comparison to ions. J_c is related to the electron concentration n_e , and drift speed v , by

$$J_c = n_e v e \quad (4).$$

For night-time conditions during which no photo-ionisation occurs, the electron concentration at 70-80 km altitude is $n_e \sim 1 \times 10^7 \text{ m}^{-3}$ (Cummer et al., 1998; Friedrich and Rapp, 2009); assuming that $J_c = 2 \text{ pA m}^{-2}$, v is therefore 4.5 km hr^{-1} . By drift speed effects alone (i.e. neglecting any other production and loss terms in the continuity equation), a 20% regional change in J_c would therefore cause a $\sim 10 \text{ km}$ variation between disturbed and undisturbed regions after 12 hours. The detection of such height changes could be made using remote radio frequency observations of the lower ionosphere. If, for example, the charge passing upwards slightly changed the effective position of the lower boundary of the ionosphere, the waveguide properties would be changed. This would modulate the waveguide cut-off frequency f_c , given by Budden (1962) as

$$f_c = \frac{c}{2h} \quad (5),$$

where h is the effective height and c the speed of light; this relation is plotted in Figure 4. The perturbations to h of $\sim 10 \text{ km}$ per 12 hours represent a $\sim 13 \%$ change in $f_c \sim 2 \text{ kHz}$, which would be readily detectable. This explanation fully accounts for the DEMETER results (Nemec et al., 2009) and is also similar to the pre-seismic changes in f_c reported by Pulinets (1998).

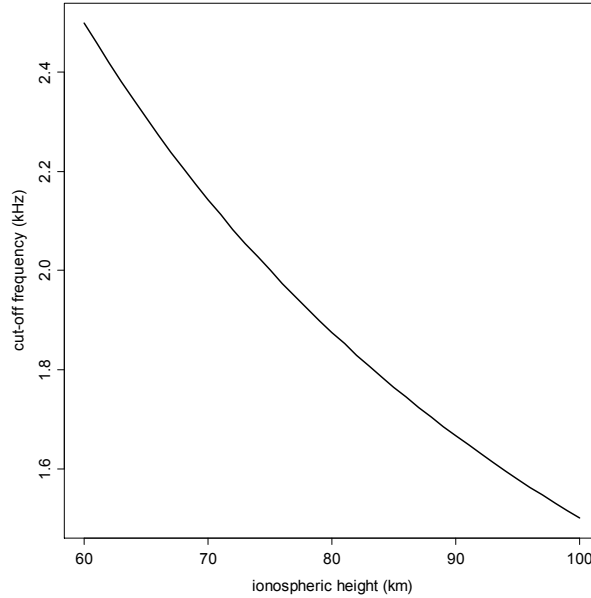


Figure 4. Variation of the cut-off frequency for Earth-ionosphere waveguide propagation (equation 5), as a function of the height of the ionosphere.

4. Predicted effects of such changes

From these considerations, it is expected that changes in surface radon ionisation will modify the surface atmospheric electricity conditions, and, potentially, the lower ionospheric properties, via the weak fair weather conduction current carrying negative charge upwards throughout the troposphere and stratosphere. Figures 3c and d summarise the expected effects

of surface radon changes, first in the surface PG (Figure 3c), and secondly in the ionospheric cut-off frequency f_c after 12 hours (Figure 3d). The surface PG change should be detectable using conventional atmospheric electricity instrumentation, and is consistent with the observations of Kondo (1968) who measured a 10-20% decrease in the PG before earthquakes. Figure 3 also includes estimates of the typical variability of these quantities, using atmospheric electricity measurements from clean (Harrison and Nicoll, 2009) and polluted (Harrison and Ingram, 2005) sites, and information on ionospheric variability (Reuveni and Price, 2009).

It should be noted that there is substantial natural ionospheric variability due to solar and geomagnetic effects (e.g., Hargreaves, 1992) and to atmospheric wave or tidal phenomena, much of which is unexplained (Rishbeth, 2006), and some of which has even been attributed to earthquakes (Pulinets, 1998; Kazimirovsky et al., 2003; Rishbeth, 2006). Using solely ionospheric measurements for earthquake prediction therefore brings a risk of incorrect predictions of events (false positives) from natural fluctuations. If the mechanism proposed here does indeed provide a practical basis for earthquake prediction, detecting the combination of changes expected in both surface atmospheric electricity and in ionospheric parameters should be used to increase the robustness of the prediction. Experience in urban atmospheric electricity monitoring has been obtained over two centuries of observations (Aplin et al, 2008; Harrison 2009; Harrison and Aplin, 2003) and hence the electrical characteristics of polluted air are well understood. Direct, durable current density measurement instrumentation is also practicable (e.g. Bennett and Harrison, 2009). Further experimental work would, however, be needed to investigate the timescales associated with the ionospheric response to surface radon changes.

Experiments to investigate this suggested mechanism further could measure the cut-off frequency of atmospherics (sferics, for short) from lightning discharges at night. These signals, known as tweeks, propagate in the Earth-ionosphere waveguide over distances of between 1000 and 5000 km (Kumar et al., 2008). Their cut-off frequency is usually seen at ~ 1.8 kHz (Cummer et al., 1998), there being an absence of energy at frequencies just below the cut-off frequency. As demonstrated by Figure 4, the cut-off frequency is inversely proportional to the ionospheric height: f_c is therefore reduced in the middle of the night, when the ionosphere is higher than during the day. Reeve and Rycroft (1972) studied tweeks received during a solar eclipse; they found systematic cut-off frequency changes before and after the maximum eclipse effect, having made allowance for the ionospheric time constant.

In the proposed experiment, these ELF/VLF signals would have to have propagated to a suitably located ELF/VLF receiver (e.g., Fullekrug, 2010) over a region where enhanced radon emissions are occurring prior to a large earthquake. For the best results several receivers around a seismically active area, such as Japan, should be deployed. The tweeks will propagate in all directions away from the lightning sources, which occur predominantly at low to medium latitudes, so that it would be most effective to position the majority of the receivers poleward of the seismically active area, and fewer equatorward of it. The data analysis approach used by Reuveni and Price (2009) could be suitable here. Another VLF radio propagation experiment observing both the amplitude and the phase of signals propagating in the Earth-ionosphere waveguide could involve transmitters used for submarine communications, such as the Omega system, or similar systems operating around the world. Using such a method, Shvets et al. (2004) detected wave-like anomalies with periods of a few hours 1 to 3 days before moderately strong earthquakes. Also medium frequency (MF) radars, which are good at investigating lower ionospheric changes, would provide

complementary observations; the Middle and Upper atmosphere radar in Japan (see Oliver et al., 1994) would be most suitable for this purpose. More elaborate experiments could involve incoherent scatter radar, or rocket launches, as discussed by Friedrich and Rapp (2009). We hope that this paper may stimulate a variety of such experimental studies.

Acknowledgements

The ideas presented here developed from discussions stimulated by the 2009 Japanese Geosciences Union meeting, and we are each most grateful to our Japanese atmospheric electricity colleagues for invitations to speak at that meeting. We also acknowledge the assistance of Prof M. Kamogawa (Tokyo Gakugei University) and Ms E. Pope with the literature search and the very helpful contributions of two reviewers.

References

- Anderson R. V., 1977, Atmospheric electricity in the real world. In Dolezalek, H. and R. Reiter (eds), *Electrical Processes in Atmospheres*, Steinkopf Verlag
- Aplin K.L., R.G. Harrison and M.J. Rycroft, 2008, Investigating Earth's atmospheric electricity: a role model for planetary studies *Space Science Reviews* 137, 11-27 doi: 10.1007/s11214-008-9372-x
- Bennett A.J. and R. G. Harrison, 2009, Surface measurement system for the atmospheric electrical vertical conduction current density, with displacement current correction, *J. Atmos. Solar-Terr. Phys.*, 70, 1373-1381, doi: 10.1016/j.jastp.2008.04.014
- Budden K. G., 1962, *The waveguide mode theory of wave propagation*, Logos Press, London
- Chalmers J. A., 1965, *Atmospheric electricity*, 2nd edition, Pergamon Press, Oxford
- Cleveland W., 1981, LOWESS: A Program for Smoothing Scatterplots by Robust Locally Weighted Regression, *The American Statistician*, 35 (1), 54
- Cummer S. A., U. S. Inan and T. F. Bell, 1998, Ionospheric D region remote sensing using VLF radio atmospherics, *Radio Sci.*, 33, 6, 1781-1792
- Davis C. J. and C. G. Johnson, 2005, Lightning-induced intensification of the ionospheric sporadic E layer, *Nature*, 435, 799-801, doi:10.1038/nature03638
- Friedrich M. and M. Rapp, 2009, News from the lower ionosphere: A review of recent developments, *Surv. Geophys.*, 30, 525-559
- Freund F.T., I.G. Kulahci, G. Cyr, J. Ling, M. Winnick, J. Tregloan-Reed and M. Freund, 2009, Air ionization at rock surfaces and pre-earthquake signals, *J. Atmos. Sol-Terr. Phys.* 71, 1824-1834
- Fujiwara H., M. Kamogawa, M. Ikeda, J. Y. Liu, H. Sakata, Y. I. Chen, H. Ofuruton, S. Muramatsu, Y. J. Chuo and Y. H. Ohtsuki, 2004, Atmospheric anomalies observed during earthquake occurrences, *Geophys. Res. Lett.*, 31, L17110, doi:10.1029/2004GL019865
- Fullekrug M., 2010, Wideband digital low-frequency radio receiver, *Meas. Sci. Technol.*, 21, doi:10.1088/0957-0233/21/1/015901
- Harrison R.G., 2009, Two daily smoke maxima in eighteenth century London air, *Atmos. Environ.*, 43, 1364-1366, <http://dx.doi.org/10.1016/j.atmosenv.2008.11.034>
- Harrison R.G. and K.L. Aplin, 2003, Nineteenth century Parisian smoke variations inferred from atmospheric electrical observations, *Atmos. Env.*, 37, 5319-5324, doi: 10.1016/j.atmosenv.2003.09.042
- Harrison R. G. and A. J. Bennett, 2007, Multi-station synthesis of early twentieth century surface atmospheric electricity measurements for upper tropospheric properties, *Adv. Geosci.*, 13, 17-23
- Harrison R. G. and K. S. Carslaw, 2003, Ion-aerosol-cloud processes in the lower atmosphere, *Rev. Geophys.*, 41, 3, 1012, doi:10.1029/2002RG000114
- Harrison R. G. and W. J. Ingram, 2005, Air-earth current measurements at Kew, London, 1909-1979, *Atmos. Res.*, 76, 1-4, 49-64, doi:10.1016/j.atmosres.2004.11.022
- Harrison R. G. and K.A. Nicoll, Air-earth current density measurements at Lerwick; implications for seasonality in the global electric circuit, *Atmos. Res.*, 89, 1-2, 181-193, doi:10.1016/j.atmosres.2008.01.008
- Harrison R. G. and H. Tammert, 2008, Ions in the terrestrial atmosphere and other solar system atmospheres, *Space Science Reviews*, 137, 107-118, doi: 10.1007/s11214-008-9356-x
- Hargreaves J.K., 1992, *The solar-terrestrial environment*, Cambridge University Press
- Hayakawa M., 2006, Electromagnetic phenomena associated with earthquakes, *IEEJ Trans. FM.*, 126, 4, 211-214

Hegai V. V., V. P. Kim and J. Y. Liu, 2006, The ionospheric effect of atmospheric gravity waves excited prior to strong earthquake, *Adv. Space Res.*, 37, 4, 653-659, [doi:10.1016/j.asr.2004.12.049](https://doi.org/10.1016/j.asr.2004.12.049)

Kamogawa M., 2006, Preseismic Lithosphere-Atmosphere-Ionosphere Coupling, *EOS Trans*, 87, 40, 417-424

Kamogawa M., J. Y. Liu, H. Fujiwara, Yb-Jung Chuo, Yi-Ben Tsai, K. Hattori, T. Nagao, S. Uyeda and Y. H. Ohtsuki, 2004, Atmospheric field variations before the March 31, 2002 M6.8 earthquake in Taiwan, *Terr. Atmos. Ocean. Sci.*, 15 (3), 397-412

Kazimirovsky E., M. Herraiz and B. A. de la Morena, 2003, Effects on the ionosphere due to phenomena occurring below it, *Surv. Geophys.*, 24, 139-184

Kim V.P., V.V. Khagai and P.V. Illich-Svitych, 1994, On one possible ionospheric precursor of earthquakes, *Phys. Solid Earth.*, 30, 3, 223-226

Kondo G., 1968, The variation of the atmospheric field at the time of earthquake. *Mem. Kakioka Magnetic Observatory*, 13, 11-23

Kumar S., A. Kishore and V. Ramachandran, 2008, Higher harmonic tweek sferics observed at low latitude: estimation of VLF reflection heights and tweek propagation distance, *Ann. Geophys.*, 26, 1451-1459

Nagamoto H., T. Fukushima, Y. Ida, Y. Matsudo and M. Hayakawa, 2008, Disturbances in VHF/UHF telemetry links as a possible effect of the 2003 Hokkaido Tokachi-oki earthquake, *Natural Hazards Earth System Sci.*, 8, 813-817

Naman S., L. S. Alperovich, S. Wdowinski, M. Hayakawa and E. Calais, 2002, Comparison of simultaneous observations of the ionospheric total electron content and geomagnetic field associated with strong earthquakes, In: Hayakawa M. and Molchanov O.A. (eds), *Seismo Electromagnetics: Lithosphere-Atmosphere-Ionosphere Coupling*, pp303-308, TERRAPUB, Tokyo

Němec F., O. Santolík and M. Parrot, 2009, Decrease of intensity of ELF/VLF waves observed in the upper ionosphere close to earthquakes: A statistical study, *J. Geophys. Res.*, 114, A04303, [doi:10.1029/2008JA013972](https://doi.org/10.1029/2008JA013972)

Ohta K., K. Umeda, N. Watanabe and M Hayakawa., 2002, Relationship between ELF magnetic fields and Taiwan earthquake, In: Hayakawa M. and Molchanov O.A. (eds), *Seismo Electromagnetics: Lithosphere - Atmosphere - Ionosphere Coupling*, pp233-237, TERRAPUB, Tokyo

Oliver W. L., S. Fukao, S. Y. Yamamoto, T. Takami, M. D. Yamanaka, M. Yamamoto, T. Nakamura and T. Tsuda, 1994, Middle and upper atmosphere observations of ionospheric density gradients produced by gravity wave packets, *J. Geophys. Res.*, 99, 6321-6329

Pierce E., 1976, Atmospheric electricity and earthquake prediction, *Geophys. Res. Lett.*, 3, 3, 185-188

Pulinets S., 1998, Seismic activity as a source of the ionospheric variability, *Adv. Space Res.* 22, 6, 903-906

Reeve C. D. and M. J. Rycroft, 1972, The eclipsed lower ionosphere as investigated by natural very low frequency radio signals, *J. Atmos. Terr. Phys.*, 34, 667-672

Reuveni Y. and C. Price, 2009, A new approach for monitoring the 27-day solar rotation using VLF radio signals on the Earth's surface, *J. Geophys. Res.*, 114, A10306, [doi:10.1029/2009JA014364](https://doi.org/10.1029/2009JA014364).

Rishbeth H., 2006, F-region links with the lower atmosphere? *J. Atmos. Solar-Terr. Phys.*, 68, 469-478

Rycroft M.J., 2006, Electrical processes coupling the atmosphere and ionosphere: An overview, *J. Atmos. Solar-Terr. Phys.*, 68, 445-456

Rycroft M.J., S. Israelsson and C. Price, 2000, The global atmospheric electric circuit, solar activity and climate change, *J. Atmos. Solar-Terr. Phys.*, 62, 1563-1576

Rycroft M. J., A. Odzimek, N. F. Arnold, M. Fullekrug, A. Kulak and T. Neubert, 2007, New model simulations of the global atmospheric electric circuit driven by thunderstorms and electrified shower clouds: The roles of lightning and sprites, *J. Atmos. Solar-Terr. Phys.*, 69, 2485-2509

Rycroft M. J., R. G. Harrison, K. A. Nicoll and E. A. Mareev, 2008, An overview of Earth's global electric circuit and atmospheric conductivity, *Space Science Reviews*, 137, 83-105, [doi: 10.1007/s11214-008-9368-6](https://doi.org/10.1007/s11214-008-9368-6)

Schekotov A. Y., O. A. Molchanov, M. Hayakawa, E. N. Fedorov, V. N. Chebrov, V. I. Sinitsin, E. E. Gordeev, G. G. Belyaev and N. V. Yagova, 2007, ULF/ELF magnetic field variations from atmosphere induced by seismicity, *Radio Sci.*, 42, RS6S90, [doi:10.1029/2005RS003441](https://doi.org/10.1029/2005RS003441)

Shvets A. V., M. Hayakawa, O. A. Molchanov and Y. Ando, 2004, A study of ionospheric response to regional seismic activity by VLF radio sounding, *Phys. Chem. Earth*, 29, 4-9, 627-637, [doi:10.1016/j.pce.2003.08.063](https://doi.org/10.1016/j.pce.2003.08.063)

Surkov V.V., O.A. Pokhotelov, M. Parrot and M. Hayakawa, 2006, On the origin of stable IR anomalies detected by satellites above seismo-active regions, *Phys. Chem. Earth*, 31, 164-171, 2006, [doi:10.1016/j.pce.2006.02.020](https://doi.org/10.1016/j.pce.2006.02.020)

Yasuoka Y. and M. Shinogi, 1997, Anomaly in atmospheric radon concentration: a possible precursor of the 1995 Kobe, Japan, earthquake, *Health Physics*, 72, 5, 759-761

Yasuoka Y., G. Igarashi, T. Ishikawa, S. Tokonami and M. Shinogi 2006, Evidence of precursor phenomena in the Kobe earthquake obtained from atmospheric radon concentration, *App. Geochem*, 21, 6, 1064-1072, [doi:10.1016/j.apgeochem.2006.02.019](https://doi.org/10.1016/j.apgeochem.2006.02.019)

Yonaiguchi N., Y. Ida and M. Hayakawa, 2007, On the statistical correlation of over-horizon VHF signals with meteorological radio ducting and seismicity, *J. Atmos. Solar-Terr. Phys.*, 69, 661-674